U.P.B. Sci. Bull., Series B, Vol. 87, Iss. 4, 2025 ISSN 1454-2331

VALORIZATION OF MINING TAILINGS BY ADSORPTION ON CALCIUM ALGINATE

David-Daniel NEAGU[1], Claudia Maria SIMONESCU*[2], Ioan CĂLINESCU[3], Carmen DELEANU[4], Mădălina Andreea PANDELE[5]

The research carried out aims at the extraction of Fe(III), Al(III) and Mg(II) ions from aqueous solutions with content similar to mine tailings by adsorption on calcium alginate. Calcium alginate prepared by precipitation from sodium alginate in the presence of microwaves (MW) and ultrasound (US) was used as adsorbent. Batch tests were carried out to recover Mg(II) ions from single and ternary solutions that also contain Al(III) and Fe(III) ions in concentrations like those identified in the mine tailings from the Sasca Montană area. The decrease in retention efficiency was found in the series: Mg(II) > Fe(III) > Al(III) in the case of the ternary solution compared to the monocomponent solutions. This decrease explains the antagonistic effect shown by each of the three metal ions tested. The pH value was monitored before and after the retention process and XPS analyzes were performed to establish the nature of the mechanism involved in the retention process. The results obtained revealed that the ion exchange process takes place by replacing Ca(II) ions with Mg(II), Al(III) and Fe(III) ions. Desorption tests of the tested metal ions were carried out using 0.01M HCl as a desorption agent. The results obtained after the first adsorption-desorption cycle indicate values of the efficiency of the desorption process that vary in the range of 75.08±2 - 94.72±1.31%.

Keywords: mine tailings, Mg(II), Al(III) and Fe(III) recovery, calcium alginate, microwaves, ultrasounds, desorption

1. Introduction

The mining industry in Romania has a long tradition [1]. However, its negative impact on the environment is relevant. The mine waste are characterized by high concentrations of metallic and metalloid contaminants which are highly

---

[1] Student, Dept. of Analytical Chemistry and Environmental Engineering, National University of Science and Technology POLITEHNICA Bucharest, Romania, e-mail: davidneagu.oto@gmail.com

[2] Prof., Dept. of Analytical Chemistry and Environmental Engineering, National University of Science and Technology POLITEHNICA Bucharest, Romania, e-mail: claudia.simonescu@upb.ro

[3] Prof., Dept. of Bioresources and Polymer Science, National University of Science and Technology POLITEHNICA Bucharest, Romania, e-mail: ioan.calinescu@upb.ro

[4] Eng., KEMCRISTAL SRL, Romania, e-mail: carmen_deleanu@yahoo.com

[5] Assoc. Prof., Dept. of Analytical Chemistry and Environmental Engineering, National University of Science and Technology POLITEHNICA Bucharest, Romania, e-mail: madalina.pandele@upb.ro

harmful and toxic to the plants, land, and human life [2]. Therefore, the efficient recovery of metals from mine tailings is a serious problem and a great challenge [1]. One of the concerns is related to tailings ponds or tailing dumps that have remained over large areas and are an aggressive source, leading to changes in soil, water, air and ecosystems. The main issue is the pollution of natural waters with acidic effluents with a relatively high metal content from mining waste storage areas [1].

The European Union creates the Strategic Implementation Plan for the European Innovation PartnerShip on Raw Materials and the Raw Materials Initiative. It is based on three pillars: (i) guaranteeing access to raw materials; (2) determining the conditions for a sustainable supply of raw materials from European sources; (3) boosting resource efficiency and promoting recycling to reduce the consumption of raw materials and reduce dependence on imports [3].

The national strategy includes the recovery and capitalization of metals based on the circular economy concept [1, 4, 5]. The circular economy involves the development of technologies to the extent that the economic effort is covered by the added value associated with new applications of reuse of mining waste [6]. By this, natural resources are maintained and protected [6].

Mining waste is valuable due to its metal content and can be exploited and valued through the development of innovative technologies for the recovery of useful elements to be reused in areas of strategic importance, thus obtaining new products and materials with high added value. Physical, thermal and chemical methods have been applied to recover the metal from mining waste. For example, the flotation has been used as a versatile method to recover cobalt [7], copper [8] and tin [9] from different tailing types. Different separation technologies based on the density and size difference have been applied to recover zinc [10] chromium [11], and lead [10]. Magnetic separation has shown potentiality to recover manganese [12], iron [13], chromium [14], and titanium [15] from tailings. Tin [16] and gold [17] have been recovered from tailings by pyrometallurgical processes. Hydrometallurgical technologies based on the treatment of mine tailings with aqueous solutions of leaching, reducing, oxidizing, and complexing agents are considered versatile options for numerous valuable metals [18]. For example, zinc [19], copper [20], gold [21] has been recovered from tailings by hydrometallurgical technologies. The metal is transformed into a dissolved form by hydrometallurgical processing, and it should be extracted from the leachate. Chemical precipitation, ion exchange, solvent extraction, electrolysis and/or crystallization can be used for the recovery of metals from leachate [16]. The main factors for choosing the technique for recovering metals from mining waste, wastewater and aqueous effluents are: (i) type of waste, (ii) the content of metal ions in wastewater/waste, (iii) the storage material, (iv) operational cost, and (v) the problem of disposal of residual metal sludge.

Due to the numerous advantages of adsorption using biomaterials such as alginates [22], the main objective of the present research study is to extract Fe(III), Al(III) and Mg(II) ions from single and ternary aqueous solutions with content similar to mine tailings from the Sasca Montană area by adsorption on calcium alginate. The recovery of Mg(II) ions from mining tailings is pursued because the EU imports over 90% of the magnesium required from China, which is essential to produce light aluminum alloys used in vehicles and packaging. The effectiveness and selectivity of calcium alginate will be analyzed.

2. Experimental part

Materials and testing equipments

Calcium alginate prepared by precipitation from sodium alginate in the presence of microwaves (MW) and ultrasound (US) was used as adsorbent. The synthesis procedure and its characterization is shown in our previous study [23].

Stock solutions of metal ions with a concentration of 1000 mg/L were prepared using $AlCl_3 \cdot 6H_2O$, $FeCl_3$ and $MgCl_2 \cdot 6H_2O$ from Merck, Germany. These solutions were diluted to prepare 175 mg/L Al(III), 125 mg/L Fe(III), and 50 mg/L Mg(II) concentration solutions to be used in the adsorption tests. Single and ternary solutions containing these metal ions have been prepared.

Quantitative determination of Al(III)/Fe(III)/Mg(II) ions was performed using an AAnalyst 400 atomic absorption spectrometer (Perkin Elmer, USA), and pH was determined with an Agilent 3200P laboratory pH meter. FT-IR spectra were recorded on a Bruker Tensor27 spectrophotometer with an ATR device.

The surface's structures for calcium alginate before and after adsorption of Al(III)/Fe(III)/Mg(II) ions were studied by X-ray Photoelectron Spectroscopy (XPS) using a K-Alpha instrument from Thermo Scientific, with a mono-chromated Al Ka source (1486.6 eV), at a bass pressure of 2×10^{-9} mbar. The pass energy for the survey spectra and high-resolution spectra were 200 eV and 20 eV respectively. The deconvolution of C1s, O1s, Mg1s, Ca2p, Fe2p, Al2p spectra was performed for the samples by using a Shirley background and a Gaussian-Lorentzian function.

Batch tests were performed to retain Al(III)/Fe(III)/Mg(II) ions from single and ternary aqueous solutions at 20 °C using a GFL 3031 shaking incubator system at 175 rpm. 100 mL metal ions solutions have been contacted with 0.1 g of calcium alginate for 8 hours. After that, samples have been filtered and the residual concentration of metal ions has been determined.

The adsorption capacity of Al(III)/Fe(III)/Mg(II) ions was calculated using the equation below, (1):

$$\mathrm{Q} = \frac{(C_0 - C_t) \cdot V}{m} \tag{1}$$

where: Q defines the removal capacity, expressed by the amount of Al(III)/Fe(III)/Mg(II) ions retained on the calcium alginate mass (mg/g); C_0 represents the initial concentration of Al(III)/Fe(III)/Mg(II) ions in the solution (mg/L); C_t is the concentration of Al(III)/Fe(III)/Mg(II) ions at a certain time t (or at different pH values) (mg/L); V defines the volume of Al(III)/Fe(III)/Mg(II) ion solution (L); m represents the mass of calcium alginate (g).

Desorption tests were carried out on calcium alginate loaded with retained metal ions using 0.01M HCl solution (100 mL). The contact time between the calcium alginate loaded with retained metal ions and 0.01M HCl solution was fixed at 8 hours. Experiments regarding adsorption and desorption were performed in triplicate, with a maximum standard error of 5%.

3. Results and discussion

Calcium alginate characterization

Calcium alginate (AlgCa) prepared in the presence of microwaves (MW) and ultrasound (US) has been already characterized in our previous research [23]. To demonstrate the higher capacity of this adsorbent for metal ions adsorption we will present and discuss only the results of the Scanning Electron Microscopy (SEM) analysis. The SEM images of the calcium alginate sample used in tests recorded at different magnifications are illustrated in Fig. 1.

Scanning electron microscopy images at different magnifications (Fig. 1(A)-(F)) reveal AlgCa particles with irregular surface and visible cracks and holes. The microwave heating combined with ultrasounds are responsible for the cracks and holes on the AlgCa [23]. The roughness of the surface and craks and holes will determine the incraese of the specific surface area and the increase of the retention capacity of metal ions [23].

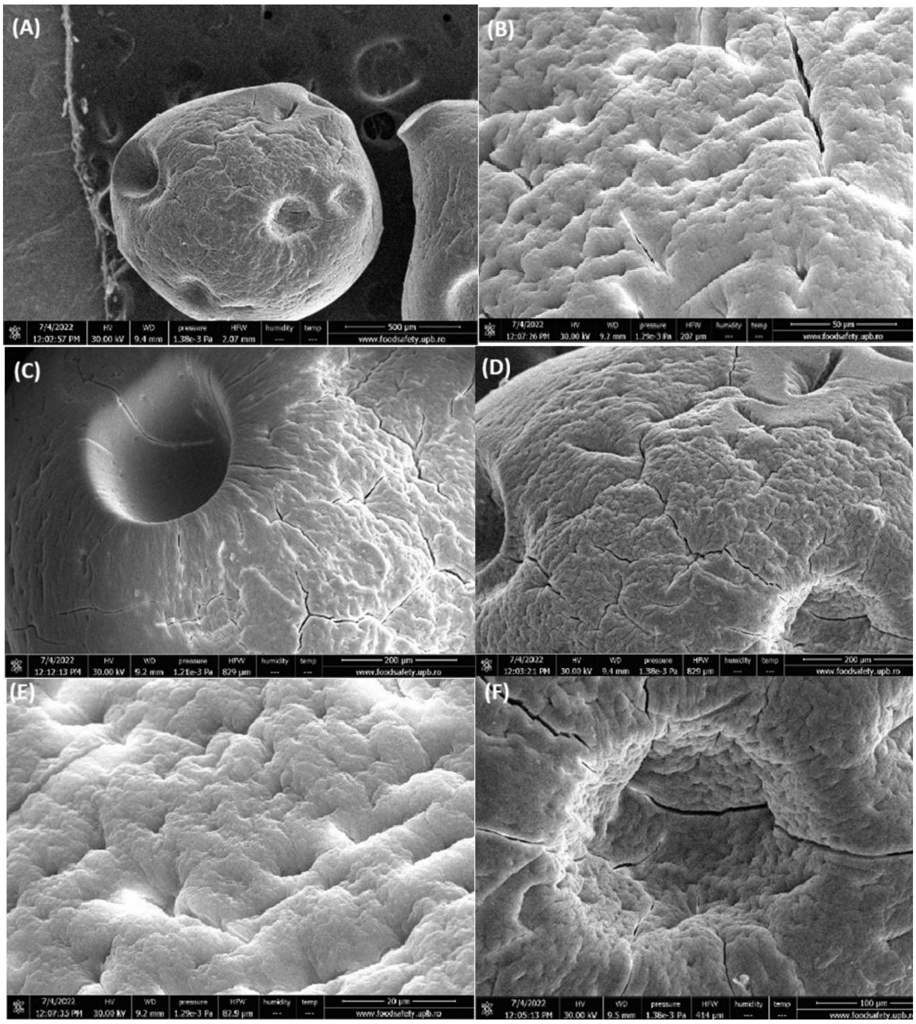

Fig. 1. SEM images of the calcium alginate sample recorded at different magnifications: (A) 200X; (B) 10.000X; (C) 5000X; (D) 5000X; (E) 20.000X; (F) 2000X

Adsorption studies

The results related to the removal eficiency of Al(III)/Fe(III)/Mg(II) ions from single and ternary solutions are shown in Fig. 2. The removal eficiency (E) was determined by using the equation (2):

$$\mathrm{E} = \frac{(C_0 - C_t)}{C_0} \times 100 \tag{2}$$

where: E defines the removal efficiency, (%); C_0 represents the initial concentration of Al(III)/Fe(III)/Mg(II) ions in the solution (mg/L) and C_t is the concentration of metal ions at a certain time t (mg/L).

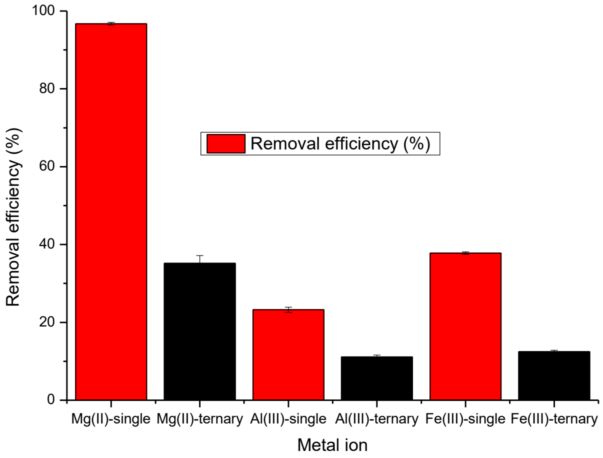

Fig. 2. The calcium alginate removal efficiency of Al(III)/Fe(III)/Mg(II) ions from single and ternary solutions

Fig. 3 highlights the adsorption capacity of AlgCa in the process of the Al(III)/Fe(III)/Mg(II) ions retention from single and ternary solutions.

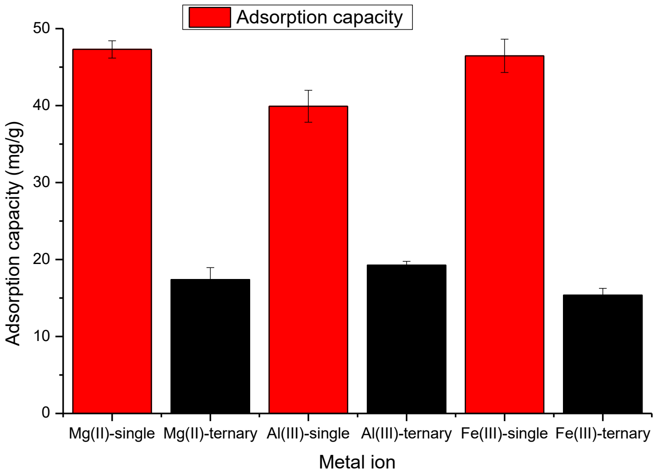

Fig. 3. The calcium alginate adsorption capacity of Al(III)/Fe(III)/Mg(II) ions from single and ternary solution

In the case of single solutions, it can be observed from Figs. 2 and 3 a variation of the removal efficiency and adsorption capacity in the series: Mg(II) > Fe(III) > Al(III). This variation can be explained based on the difference between ionic radii, hydrated ion radii and electronegativity. The values of these properties of metal ions targeted are shown in Table 1. However, the Ca(II) ions have higher ion radius and lower radius of the hydrated ion then Mg(II), Al(III) and Fe(III), the ion exchange mechanism involved can be explained by the differences between the electronegativity of these metal ions and the electronegativity of the Ca(II) [24].

Table 1.

Metal ions properties [23-26]

Metal ion	Ion radius (Å)	Radius of the hydrated ion (nm)	Electronegativity
Ca(II)	1.06	0.412	1
Mg(II)	0.72	0.428	1.31
Al(III)	0.54	0.475	1.61
Fe(III)	0.64	0.451	1.83

Considering the ionic radius, it was shown that a metal ion with a larger ionic radius is favorable to interact with the functional groups of the ion exchanger [24]. Metal ions with small, hydrated ion radius will interact more strongly with the adsorbent surface, and metal ions with higher electronegativity will be retained more easily than metal ions with lower electronegativity [24]. Mg(II) ion has larger ion radius and small hydrated ion radius compared to Fe(III) and Al(III) and it interacts more strongly with the carboxyl and hydroxyl groups in alginate because it can more easily access active sites.

In the case of the ternary solution, the following are observed:

(i) there is a decrease in retention efficiency in series: Mg(II) > Fe(III) > Al(III);
(ii) in the case of Mg(II), the retention efficiency decreases by 61.58% (compared to the retention from the single solution);
(iii) in the case of Al(III), the retention efficiency decreases by 12.12% (compared to the retention from the single solution);
(iv) in the case of Fe(III), the retention efficiency decreases by 25.37% (compared to the retention from the single solution);
(v) the decrease of both the retention efficiency and the retention capacity of each metal ions in the presence of the other two metal ions explain the antagonistic effect manifested by each of the three metal ions tested.
(vi) the greatest decrease in retention efficiency recorded in the case of Mg(II) demonstrates the strong antagonistic effect manifested by Fe(III) and Al(III) ions.

Desorption experiments

Desorption tests were carried out on calcium alginate loaded with retained metal ions using 0.01M HCl solution (100 mL).

The desorption capacity and desorption efficiency are calculated with the formulas (3) and (4):

$$Q_{e\,des} = \frac{C_{des} \cdot V}{m} \tag{3}$$

$$D = \frac{Q_{e\,des}}{Q_{e\,ads}} \times 100 \tag{4}$$

where: $Q_{e\ des}$ is desorption capacity of Al(III)/Fe(III)/Mg(II) ions (mg/g); C_{des}

defines the desorption concentration of Al(III)/Fe(III)/Mg(II) ions (mg/L); V – is volume of the desorption agent (L); m – represents the mass of the metal loaded adsorbent (g); D represents the desorption efficiency, (%); $Q_{e\ ads}$ is adsorption capacity of Al(III)/Fe(III)/Mg(II) ions (mg/g).

Results regarding the desorption capacity and desorption efficiency are revealed in Fig. 4 (A) and (B).

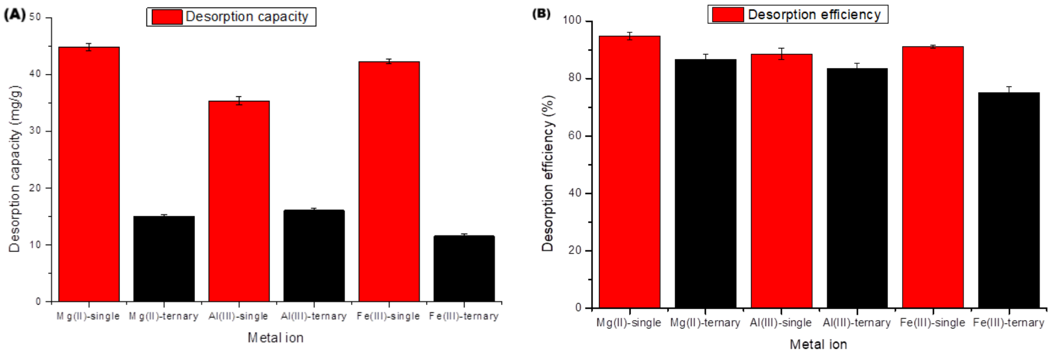

Fig. 4. (A) Desorption capacity and (B) desorption efficiency of Mg(II), Al(III) and Fe(III) retained on calcium alginate from single and ternary aqueous solutions (after the first adsorption-desorption cycle)

The results obtained after the first cycle of adsorption-desorption indicate values of the efficiency of the desorption process that vary in the range of 75.08±2 - 94.72±1.31%.

The removal mechanism

Determinations of the pH of the initial solutions and of the residual solutions were made to demonstrate the metal ion retention mechanism. The results obtained are shown in Table 2

Table 2.

The pH values of the tested solutions before and after adsorption on calcium alginate

Targeted solution	pH, pH units	Mean
Al(III) 175 mg/L – Sample 1	3.48	**3.48**
Al(III) 175 mg/L – Sample 2	3.47	
Al(III) 175 mg/L – Sample 3	3.48	
Al(III) 175 mg/L after adsorption onto AlgCa 1	3.58	**3.55**
Al(III) 175 mg/L after adsorption onto AlgCa 2	3.53	
Al(III) 175 mg/L after adsorption onto AlgCa 3	3.55	
Fe(III) 125 mg/L – Sample 1	2.49	**2.49**
Fe(III) 125 mg/L – Sample 2	2.48	
Fe(III) 125 mg/L – Sample 3	2.49	
Fe(III) 125 mg/L after adsorption onto AlgCa 1	2.52	**2.59**
Fe(III) 125 mg/L after adsorption onto AlgCa 2	2.61	
Fe(III) 125 mg/L after adsorption onto AlgCa 3	2.63	
Mg(II) 50 mg/L– Sample 1	5.48	

Mg(II) 50 mg/L– Sample 2	5.48	**5.48**
Mg(II) 50 mg/L– Sample 3	5.49	
Mg(II) 50 mg/L after adsorption onto AlgCa 1	5.47	**5.03**
Mg(II) 50 mg/L after adsorption onto AlgCa 2	4.59	
Mg(II) 50 mg/L after adsorption onto AlgCa 3	5.04	
Al(III) 175 mg/L + Fe(III) 125 mg/L + Mg(II) 50 mg/L – Sample 1	2.24	**2.24**
Al(III) 175 mg/L + Fe(III) 125 mg/L + Mg(II) 50 mg/L – Sample 2	2.24	
Al(III) 175 mg/L + Fe(III) 125 mg/L + Mg(II) 50 mg/L – Sample 3	2.23	
Al(III) 175 mg/L + Fe(III) 125 mg/L + Mg(II) 50 mg/L after adsorption onto AlgCa 1	2.33	**2.35**
Al(III) 175 mg/L + Fe(III) 125 mg/L + Mg(II) 50 mg/L after adsorption onto AlgCa 2	2.37	
Al(III) 175 mg/L + Fe(III) 125 mg/L + Mg(II) 50 mg/L after adsorption onto AlgCa 3	2.34	

The pH of the metal ions solutions (single and ternary) in contact with calcium alginate changes in the range of 0.07 – 0.45 pH units (Table 2). This modification demonstrates that the adsorption process proceeds through chemical reactions between metal ions (Al(III), Fe(III), Mg(II) and the functional groups of calcium alginate). The reactions involved are ion exchange between the metal ions from the aqueous solutions and the Ca(II) from calcium alginate.

These data were corroborated with the results obtained from FT-IR and XPS spectroscopy. The FT-IR spectra of the sodium alginate (AlgNa), calcium alginate (AlgCa), and metal loaded calcium alginate are presented in Fig. 5.

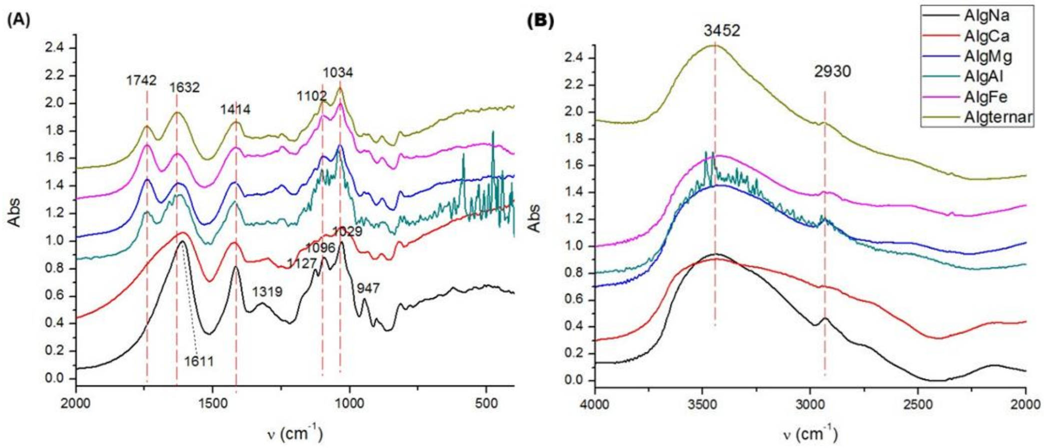

Fig. 5. FT-IR spectra of sodium alginate (AlgNa), calcium alginate (AlgCa), and metal loaded calcium alginate (A) at wavelengths 500 – 2000 cm^{-1}, and (B) at wavelengths 2000-4000 cm^{-}

All the spectra shown in Fig. 5 contain the absorption bands of the functional groups characteristic for sodium alginate. Some of them undergo slight changes attributable to the replacement of Na(I) by Ca(II), Al(III), Fe(III) and Mg(II). At around 3452 cm^{-1} is shown one broad absorption band that is assigned to the stretching vibrations of O-H bonds, while the band at 2930 cm^{-1} corresponds to the stretching vibrations of aliphatic C-H bonds [27]. The main absorption bands that confirm the formation of calcium alginate and the replacement of Ca(II) with Al(III), Fe(III) and/or Mg(II) are those characteristics to the symmetric and asymmetric stretching vibrations of the carboxylate (COO$^-$) groups [28]. In AlgNa these bands are identified at 1611 and 1319 cm^{-1}, while in AlgCa, AlgAl, AlgFe and AlgMg they are shifted to 1632 and 1414 cm^{-1} [29]. These shifts can be explained based on the modification of the radius, the atomic weight, and the charge density of the cation, when Na(I) ions are replaced by Ca(II), Al(III), Fe(III) and Mg(II). As it can be seen in Fig. 5, slight modifications are observed in the bands centred at 1319, 1096, and 1029 cm^{-1} that are attributed to the C-O stretching vibrations [27]. The FTIR results obtained are conform with the data reported in the literature [27-29]. XPS was conducted to demonstrate the ion exchange mechanism involved in metal ions removal by adsorption onto calcium alginate. In the Fig. 6 the XPS spectrum of calcium alginate used in the adsorption tests is shown.

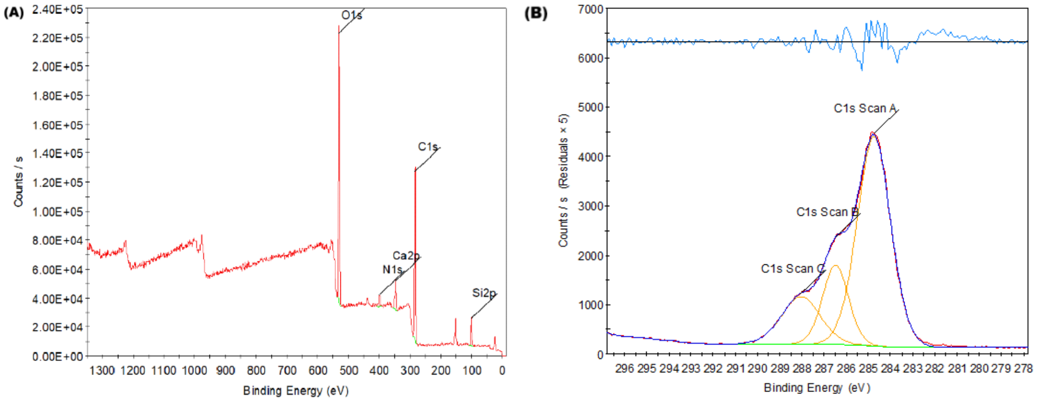

Fig. 6. Total XPS spectrum of AlgCa (A) and high-resolution XPS spectrum of carbon (B)

Fig. 6 (A) indicates the presence of O, C and Ca in the composition of calcium alginate. It is observed in the XPS spectrum, the O 1s peak at 531.29 eV and the characteristic Ca 2p3/2 peak is located at 347.47 eV being attributed to O-Ca-O bonds between calcium ions and carboxylate groups. This spectrum indicates the successful replacement of sodium ions with calcium ions. Fig. 6 (B) represents the high-resolution spectrum of C 1s, which reveals the characteristic peak at 284.74 eV. After its deconvolution, three characteristic peaks are observed at 284.99 eV (for C-C and C-H bonds), 286.7 eV (characteristic of C-O bonds) and 289.08 eV (characteristic of C=O bonds) [30]. The XPS spectrum of calcium alginate after Fe(III) removal is displayed in Fig. 7.

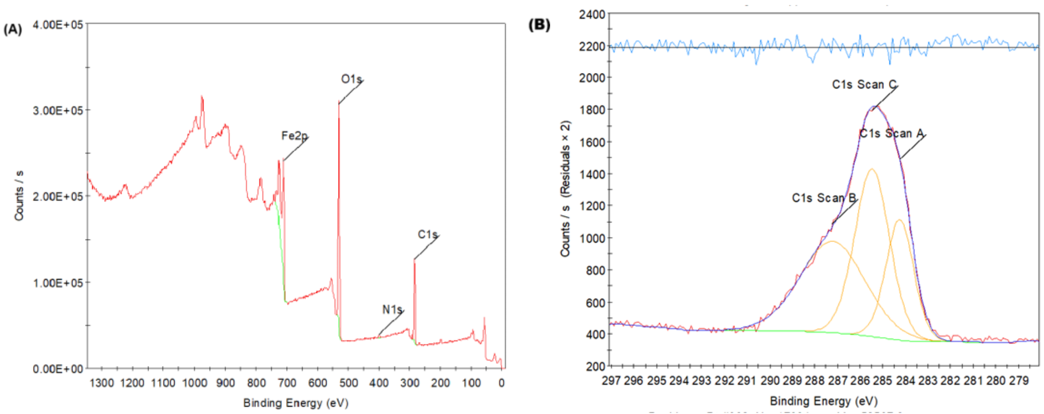

Fig. 7. Total XPS spectrum of AlgCa after Fe(III) removal (A) and high-resolution XPS spectrum of carbon (B)

Fig. 7 (A) reveals the presence of the characteristic Fe 2p peak at 710.39eV [30]. It is also observed that the characteristic O 1s peak present in calcium alginate at 531.29 eV moved to 530.33 eV after replacing Ca(II) with Fe(III). The disappearance of the characteristic Ca 2p3/2 peak at 347.47 eV is also observed. After the deconvolution of C 1s peak, three characteristic peaks are observed at 284.25 eV (for C-C and C-H bonds), 285.47 eV (characteristic of C-O bonds) and 287.21 eV (characteristic of C=O bonds). It has been remarked that all these peaks have been shifted to lower energy by replacing Ca(II) ions from calcium alginate with Fe(III) ions from the aqueous solutions [31]. This revealed that the carbon chemical environment in the calcium alginate has been changed in the Fe(III) ions removal process [31]. The adsorbent has been also characterized after Mg(II), Al(III) and Fe(III) retaining from ternary solution. The XPS spectrum recorded is visible in Fig. 8.

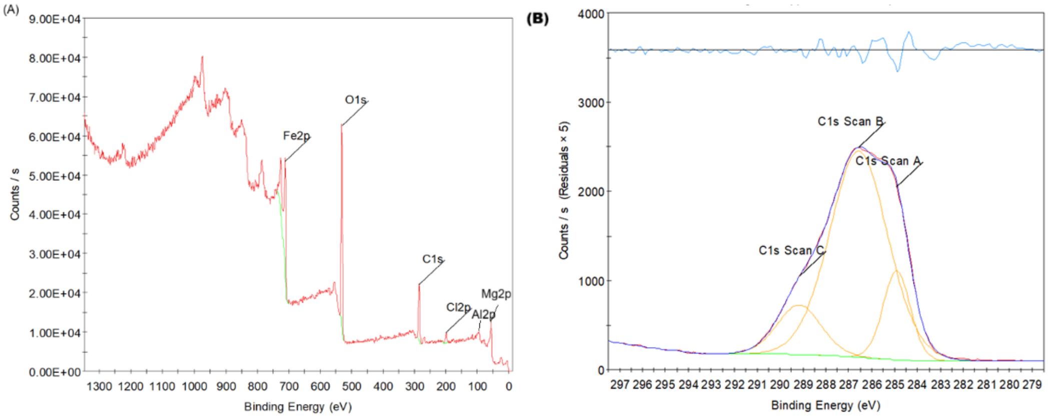

Fig. 8. Total XPS spectrum of AlgCa after Mg(II), Al(III) and Fe(III) removal from ternary solution (A) and high-resolution XPS spectrum of carbon (B)

The characteristic O 1s peak at 529.84 eV can be observed (a much larger shift compared to its position in calcium alginate) in Fig. 8 (A). The disappearance of the characteristic Ca 2p3/2 peak at 347.47 eV is also observed. The presence of the characteristic Fe 2p peak at 710.49 eV is noted [32]. The characteristic peak of magnesium Mg 1s is located at 1300 eV [33]. The two peaks at 68 eV and 73.8 eV correspond to Al2p3/2 and Al2p1/2 [33]. The characteristic peaks of C 1s are shifted from 284.99 to 284.91 eV, from 286.7 to 286.57 eV and from 289.08 to 288.17 eV by replacing Ca(II) ions from calcium alginate with Mg(II), Al(III) and Fe(III) ions from the ternary aqueous solutions [31]. This also demonstrates the changes of the carbon chemical environment in the calcium alginate by replacing with all three metal ions [31].

The high-resolution XPS spectrum of oxygen for AlgCa before and after metal ions removal (Fig. 9 A-D) has been recorded to prove the ion exchange mechanism.

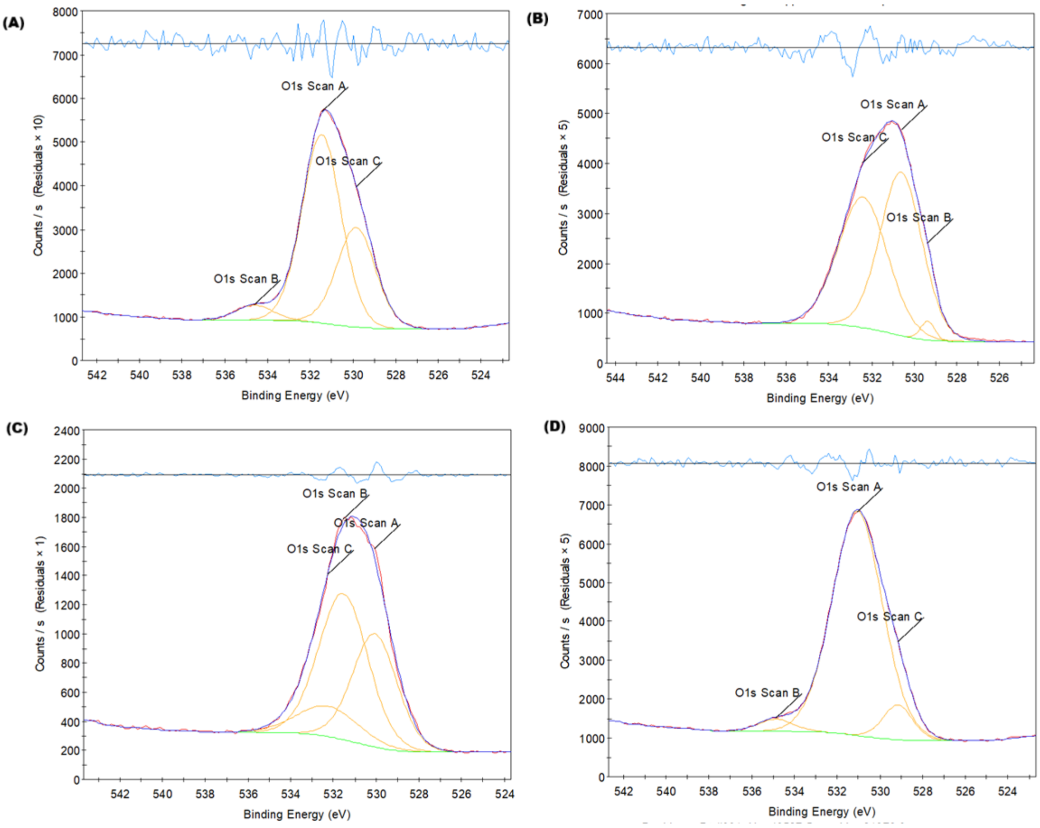

Fig. 9. The high-resolution XPS spectrum of oxygen for AlgCa (A); AlgMg (B); AlgAl (C) and AlgFe(D)

Three peaks at, 530.06, 531.54, and 534.85 eV revealed the presence of O–C=O, O–C=O and C–OH/O–C–O [34, 35] have been identified in the O 1s spectrum of AlgCa. After uptake of Mg(II), the binding energies of O atom in C=O, O=C−O, and O−H/C−O−C, were all shifted to lower binding energies (529.16, 531.05, 533.3 eV), illustrating that these groups have been involved in the retaining reaction [36]. In case of Al(III) ions it has been noticed that the binding energies of O atom were shifted to 529.76, 531.23, 532,28 eV showing bonding of Al(III) ions by O atoms of carboxyl and hydroxyl groups of alginate [35]. This observation is also valuable for Fe(III) the metal ions retained by calcium alginate. These changes in the binding energies after Mg(II)/Al(III)/Fe(III) adsorption can be due to the specific interaction between Mg(II)/Al(III)/Fe(III) and the oxygen atoms of alginate, indicating that the hydroxyl, and carboxyl groups of the alginate given a large amount of electrons to Mg(II)/Al(III)/Fe(III) to form complexes of alginate with Mg(II)/Al(III)/Fe(III) ions through cation bonding bridge and replacing Ca(II) ions from calcium alginate. These results validate the mechanism involved in metal ions removal by calcium alginate and reinforce the results of FT-IR analysis of alginate after retaining of metal ions tested [34-36].

4. Conclusions

Batch tests have been carried out to recover Mg(II) ions from single and ternary solutions that also contain Al(III) and Fe(III) ions in concentrations similar to those identified in the mine tailings from Sasca Montană area by adsorption on calcium alginate prepared in the presence of MW and US.

A decrease in retention efficiency was found in the series: Mg(II) > Fe(III) > Al(III) in the case of the ternary solution compared to the monocomponent solutions. This decrease explains the antagonistic effect shown by each of the three metal ions tested. The removal efficiency of Mg(II) from single solution is 96.75±0.34% and it decreases to 35.17±2.02 from ternary solutions. This decrease is due to the competition between Mg(II), Fe(III) and Al(III) in ternary solutions to occupy the free active sites of the calcium alginate.

The pH value was monitored before and after the retention process and XPS analyzes were performed to establish the nature of the mechanism involved in the retention process. The obtained results revealed the ion exchange process that takes place by replacing Ca(II) ions with Mg(II), Al(III) and Fe(III) ions.

Desorption tests of the tested metal ions were carried out using HCl 0.01M as a desorption agent. The results obtained after the first adsorption-desorption cycle indicate values of the efficiency of the desorption process that vary in the range of 75.08±2 - 94.72±1.31%.

Numerous research should be performed to propose the optimal uses of mine waste and to recover with high efficiency all the valuable components to be reused in areas of strategic importance.

Acknowledgments

Financial support from the Competitiveness Operational Program 2014-2020, Action 1.1.3: Creating synergies with RDI actions of the EU's HORIZON 2020 framework program and other international RDI programs, MySMIS Code 108792, Acronym project "UPB4H", financed by contract: 250/11.05.2020 is gratefully acknowledged.

REFERENCES

[1]. *A. Vasile, A.R. Milăşan, A.E. Andrei, R.N. Turcu, M.F. Drăgoescu, S. Axinte, M. Mihaly,* An integrated value chain to iron-containing mine tailings capitalization by a combined process of magnetic separation, microwave digestion and microemulsion – assisted extraction, Process Safety and Environmental Protection, **vol. 154**, 2021, pp. 118-130.

[2]. *P.I. Angulo-Bejarano, J. Puente-Rivera, R. Cruz-Ortega,* Metal and metalloid toxicity in plants: An overview on molecular aspects, Plants, **vol. 10**, no. 4, 2021, 635.

[3]. *https://single-market-economy.ec.europa.eu/sectors/raw-materials/eip_en*

[4]. Mining Strategy of Romania 2017-2035, The Ministry of Economy, first version, Jan 31, 2017

[5] *J. Mao, C. Li, Y. Pei, L. Xu*, Circular Economy and Sustainable Development Enterprises. Springer Nature Singapore Pte Ltd, 2018.

[6]. *S.K. Ghosh.* Waste Water Recycling and Management. Vol. 3. Springer, 2017.

[7]. *M.S. Lutandula, B. Maloba,* Recovery of cobalt and copper through reprocessing of tailings from flotation of oxidised ores. J. Environ. Chem. Eng. 2013, pp. 1085–1090.

[8]. *Z. Yin, W. Sun, Y. Hu, C. Zhang, Q. Guan, K. Wu,* Evaluation of the possibility of copper recovery from tailings by flotation through bench-scale, commissioning, and industrial tests. Journal of Cleaner Production **vol. 171**, 2018, pp. 1039–1048.

[9] *T. Leistner, M. Embrechts, T. Leissner, S. Chehreh Chelgani, I. Osbahr, R. Möckel, U.A. Peuker,* A study of the reprocessing of fine and ultrafine cassiterite from gravity tailing residues by using various flotation techniques. Miner. Eng. **96–97**, 2016, pp. 94–98.

[10] *A. Khalil, R. Argane, M. Benzaazoua, et al.* Pb–Zn mine tailings reprocessing using centrifugal dense media separation. Miner. Eng. **131**, 2019, pp. 28–37.

[11] *S.L. Tripathy, Y.R. Murthy, V. Singh,* Characterisation and separation studies of Indian chromite beneficiation plant tailing. Int. J. Miner. Process, **122**, 2013, pp. 47–53

[12] *X. Zhang, X. Tan, Y. Yi, et al.,* Recovery of manganese ore tailings by high-gradient magnetic separation and hydrometallurgical method. J. Occup. Med. **69**, 2017, pp. 2352–2357.

[13] *R. Bicalho da Rocha, E. Linhares Reis, J. Pancrácio Ribeiro.* Wet high-intensity magnetic separators (WHIMS) for recovering iron from tailings deposited in dams. Mineral Processing and Extractive Metallurgy (IMM Trans. Sect. C) **42** (1), 2019, 17–23.

[14] *A. Güney, G. Önal, T. Atmaca,* New aspect of chromite gravity tailings reprocessing. Minerals Engineering **14** (11), 2001, 1527–1530.

[15] *H. Zhang, J. Zeng, H. Xie, C. Guan, L. Chen*, Enhanced separation for ilmenite tailings with a novel HGMS-flotation process. Separation Science and Technology **55**, 2020, pp. 752–760.

[16] *F.A. López, I. García-Díaz, O. Rodrígues Largo, et al.* Recovery and purification of tin from tailings from the Penouta Sn–ta–Nb deposit. Minerals, **8**, 2018, 20.

[17] *P. Fu, Z. Li, J. Feng, Z. Bian*, Recovery of gold and iron from cyanide tailings with a combined direct reduction roasting and leaching process. Metals. 8, 2018, 561.

[18] *M.L. Free*, Hydrometallurgy: Fundamentals and Applications. John Wiley & Sons, Incorporated, Somerset, 2013.

[19] *S. Espiari, F. Rashchi, S.K. Sadrnezhaad*, Hydrometallurgical treatment of tailings with high zinc content. Hydrometallurgy. **82**, 2006, pp. 54–62.

[20] *M.M. Antonijevic, M.D. Dimitrijevic, Z.O. Stevanovic, S.M. Serbula, S.M. Bogdanovic*, Investigation of the possibility of copper recovery from the flotation tailings by acid leaching. Journal of Hazardous Materials **158**, 2008, pp. 23–34.

[21] *P. Altinkaya, J. Mäkinen, P. Kinnunen, E. Kolehmainen, M. Haapalainen, M. Lundström*, Effect of biological pretreatment on metal extraction from flotation tailings for chloride leaching. Minerals Engineering. **129**, 2018, pp. 47–53.

[22] *A. Miron, et. al.,* Innovative Alginate-based Hybrid Composite Beads for Heavy Metals Removal. U.P.B. Sci. Bull., Series B, Vol. 86, Iss. 1, 2024, pp. 3-18.

[23] *C.M. Simonescu, P. Chipurici, I. Călinescu, M. Vînătoru, E.N. Toma, D.C. Culiţă, V.L. Ene, T.J. Mason,* Effects of ultrasounds and microwaves on the morphology and adsorption capacity of calcium alginate. Colloids and Surfaces A: Physicochemical and Engineering Aspects. 2024, Article Number 132906.

[24] *A. Yadav, N. Bagotia, A.K. Sharma, S. Kumar*, Simultaneous adsorptive removal of conventional and emerging contaminants in multi-component systems for wastewater remediation: A critical review, Science of the Total Environment, **799**, 2021, 149500.

[25] *A. Friedrich, et al.*, Cationic Heterobimetallic Mg(Zn)/Al(Ga) Combinations for Cooperative C–F Bond Cleavage Angew. Chem. Int. Ed. **60**, 2021, 16492 – 16499

[26] *J. Duan, B. Ma, F. Liu, S. Zhang, S. Wang, Y. Kong, et al*, Coordination ability determined transition metal ions substitution of Tb in Tb-Asp fluorescent nanocrystals and a facile ions-detection approach, Nanoscale, **10**, 2018, 7526-7535

[27] *H. Daemi, M. Barikani*, Synthesis and characterization of calcium alginate nanoparticles, sodium homopolymannuronate salt and its calcium nanoparticles, Sci. Iran. **19**, 2012, 2023–2028.

[28] *C.M. Simonescu, T.J. Mason, I. Călinescu, V. Lavric, M. Vînătoru, A. Melinescu, D.C. Culiţă*, Ultrasound assisted preparation of calcium alginate beads to improve absorption of Pb^{+2} from water. Ultrasonics Sonochemistry, **68**, 2020, 105191.

[29] *T.J. Stewart, J.-H. Yau, M.M. Allen, D.J. Brabander, N.T. Flynn*, Impacts of calcium alginate density on equilibrium and kinetics of lead(II) sorption onto hydrogel beads. Colloid Polym. Sci. **287**, 2009, pp. 1033–1040.

[30] *C. Jiao, J. Xiong, J. Tao, S. Xu, D. Zhang, H. Lin, Y. Chen*, Sodium alginate/graphene oxide aerogel with enhanced strength–toughness and its heavy metal adsorption study. International Journal of Biological Macromolecules, **83**, 2016, pp. 133–141.

[31] *J. Shen, L. Kuang, W. Wei*, Fabrication of porous lightweight calcium alginate-tannic acid composite beads for enhanced heavy metal ions removal, International Journal of Biological Macromolecules, 311, 2025, 144102.

[32] *M. Liu, Q. Meng, C. Niu, Y. Wang, G. Zhou, C. Xu, Y. Liu,* Preparation and characterization of modified dual network dust suppression gel based on sodium alginate and soluble starch. Environmental Science and Pollution Research **29**, 2022, 69771–69784.

[33] *A. Chatla, et a.* Efficient Removal of Eriochrome Black T (EBT) Dye and Chromium (Cr) by Hydrotalcite-Derived Mg-Ca-Al Mixed Metal Oxide Composite. Catalysts **12**, 2022, 1247.

[34] *Z. Jing, X. Dai, X. Xian, X. Du, M. Liao, P. Hong and Y. Li*, Tough, stretchable and compressive alginate-based hydrogels achieved by non-covalent interactions, RSC Adv., **10**, 2020, 23592.

[35] *H. Luo, Y. Liu, H. Lu, Q. Fang, and H. Rong*, Efficient Adsorption of Tetracycline from Aqueous Solutions by Modified Alginate Beads after the Removal of Cu(II) Ions, ACS Omega, **6**, 9, 2021, pp 6240-6251.

[36] *N.E. Mousa, C.M. Simonescu, R.-E. Pătescu, C. Onose, C. Tardei, D. C. Culiţă, O. Oprea, De. Patroi, V. Lavric*, Pb^{2+} removal from aqueous synthetic solutions by calcium alginate and chitosan coated calcium alginate. Reactive and Functional Polymers 109 (2016) pp 137-150.